Examining Similarity and LES Models for Homogenous Variable-Density Turbulence

Omkar Shende

Buoyancy-generated turbulence is inherently complex and unsteady, as can be seen in phenomena such as the Rayleigh-Taylor instability, and yet its ubiquity in naturally occurring and mixing flows makes it particularly salient as a topic of study. A fundamental nondimensional parameter that governs such flows when they have two distinct fluids is the Atwood number, defined as

$$A = \frac{\rho_2 - \rho_1}{\rho_2 + \rho_1},$$

where $\rho_1$is the density of the lighter fluid. In the limit of zero Atwood number, the Boussinesq approximation is valid and the incompressible Navier-Stokes equations govern the system. When density differences are not negligible, however, the compressible equations must be used.

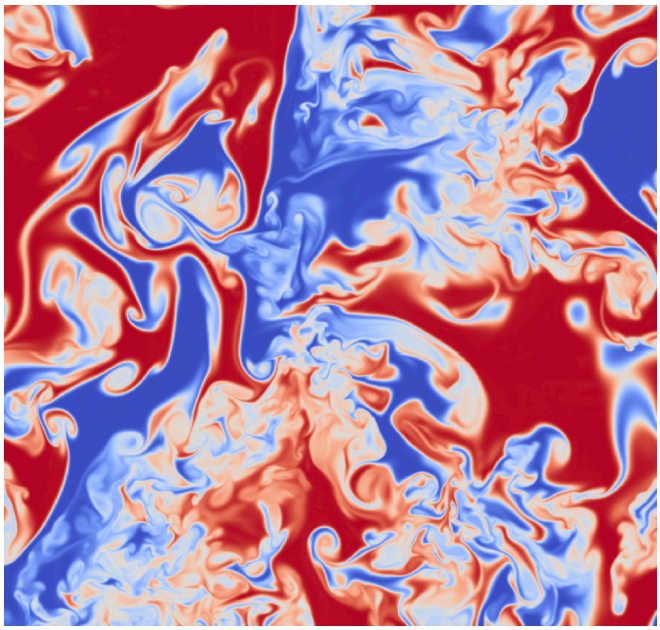

Fig. 1: Sample early time snapshot of a simulation of homogenous variable density turbulence. [3]

Homogenous variable-density (HVD) turbulence consists of a triply periodic box with zero initially imposed velocity gradients and gravity acting in one dimension normal to a box face. Such a setup yields an unsteady solution, as initially heterogeneously scattered parcels of fluid, seen in Fig. 1., will cause fluctuating buoyant forces that will move the box towards isotropy. This is an ideal test case for examining buoyancy-driven turbulence because of the multiple homogeneities.

In [1], Batchelor defines a parameter γ to characterize the anisotropy in the system, given as:

$$\gamma = \frac{2 < u_1^2 >}{< u_3^2 > + < u_2^2 >}.$$

In HIT, this parameter would be unity, but Batchelor shows this is initially about 8 in HVD flows, and it is this anisotropy that fundamentally differentiates HVD from HIT.

Using this information, [1] shows a detailed analytic derivation of universality in such flows in the Boussinesq limit. In particular, self-similarity in the evolution of HVD in intermediate times is salient when considering unsteadiness. For the box in question, we can write the governing equations for the turbulent kinetic energy (TKE) and turbulent potential energy (TPE) as:

$$\frac{1}{2}\frac{d<u^2>}{dt} = \frac{g}{\rho_0} < u_1\rho' > + \nu < \boldsymbol{u} \cdot \nabla^2 \boldsymbol{u} >$$

$$\frac{1}{2}\frac{d<\rho'^2>}{dt} = D < \rho' \nabla^2 \rho' > .$$

That is, only production and dissipation matter. Batchelor then claims that the energy transfer rate at some length L will be equal to the dissipation, simplifying both equations to

$$\frac{1}{2}\frac{d<u^2>}{dt} = \frac{g}{\rho_0} < u_1\rho' > - \frac{\alpha}{L} < u^2 >^{3/2}$$

$$\frac{1}{2}\frac{d<\rho'^2>}{dt} = -\frac{\alpha}{L} < u^2 >^{\frac{1}{2}} < \rho'^2 > ,$$

where α is some constant close to unity. Now, we define two more parameters,

$$\zeta = \frac{< \rho' u_1 >}{< \rho'^2 >< u_1^2 >} \qquad and \qquad \xi = \frac{\zeta \gamma^{1/2}}{(2+\gamma)^{1/2}},$$

allowing us to write the governing equation for the TKE as

$$\frac{1}{2}\frac{d<u^2>}{dt} = \frac{g\xi}{\rho_0} < \rho'^2 >^{1/2} - \frac{\alpha}{L} < u^2 >^{3/2}$$

This remarkably has a solution, allowing us to write, in nondimensional form, equations for both velocity and density fluctuations as

$$< U^2 >^{1/2} = \frac{\xi T}{1 + \frac{\alpha}{2}\xi T^2}$$

$$< \Theta^2 >^{1/2} = \frac{1}{1 + \frac{\alpha}{2}\xi T^2}.$$

The constants are defined through curve-fitting to numerical data and Batchelor's work was originally done on an LES grid of 128 x 128 x 128.

Using direct numerical simulation data from [3], which provides a high-quality source of low Atwood number buoyant turbulence, let's test these models. The flow is at an Atwood number of 0.05, so the Boussinesq analysis is valid. First, the right plot of Fig. 2 shows a plot of Batchelor's invariant, γ as it evolves. It starts close to the theoretical HIT value of 8 and shows a gradual, but never complete, return to almost isotropy. According to [2], most simulations created by Livescu and Ristrocelli used a density field with characteristic wavenumbers in the range $3<k<5$, and as [3] comes from the same research group, we assume the same is probably true here. In that case, the asymptotic value of ~2.5 matches closely with the value of 2.4 [1] reports for $k = 4$.

A more recent look at this problem is [2], which particularly addresses modeling concerns such as Reynolds stress alignment. In this work, a Reynolds stress anisotropy tensor can be derived as

$$b_{ij} = \frac{< u_i u_j >}{< u_k u_k >} - \frac{1}{3}\delta_{ij}.$$

if we consider the Boussinesq limit.

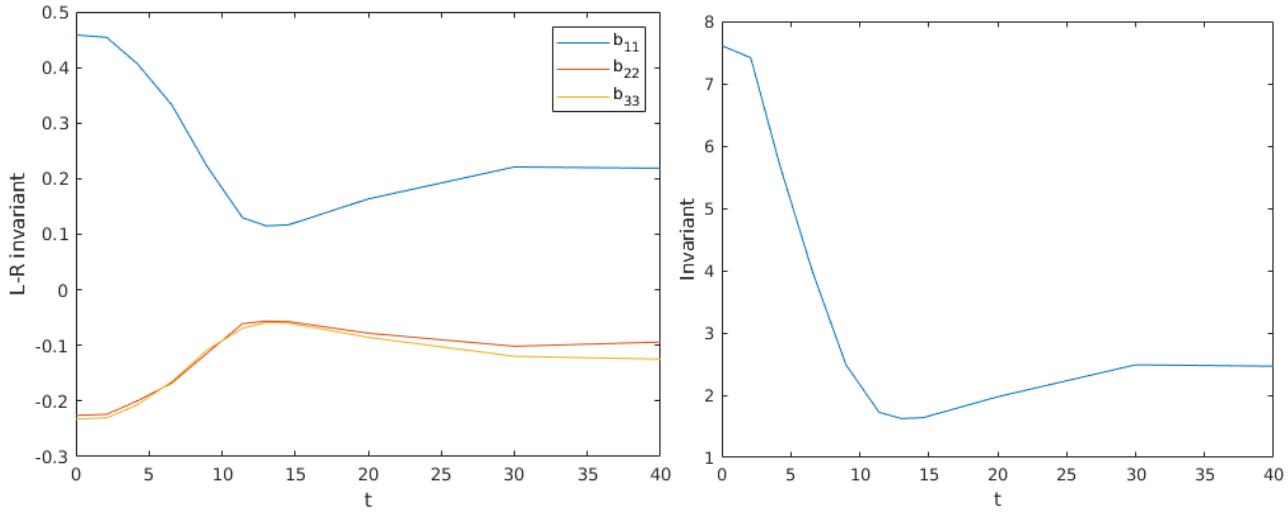

Figure 2: Livescu-Ristrocelli invariant (L) and Batchelor invariant (R)

In the left plot of Fig. 2, which shows this tensor's diagonal components, see that the majority of the buoyancy-driven production occurs in the direction aligned with the gravity vector, which points in the 1-direction. In HIT, the diagonal components of this tensor would be 0, but in this case, they are very much not. Much like with γ, we see that the flow actually backs away from isotropy as time advances. If we examine the invariant triangle for this flow scenario in Fig. 2, we see that the flow moves from the one-component point towards isotropy, before moving back towards the starting point. The entire trajectory is along the axisymmetric line, which makes

sense, and so we characterize the Reynolds stress as a prolate spheroid. While not shown here, the off-diagonal components of the Reynolds stress are much smaller than the diagonal components.

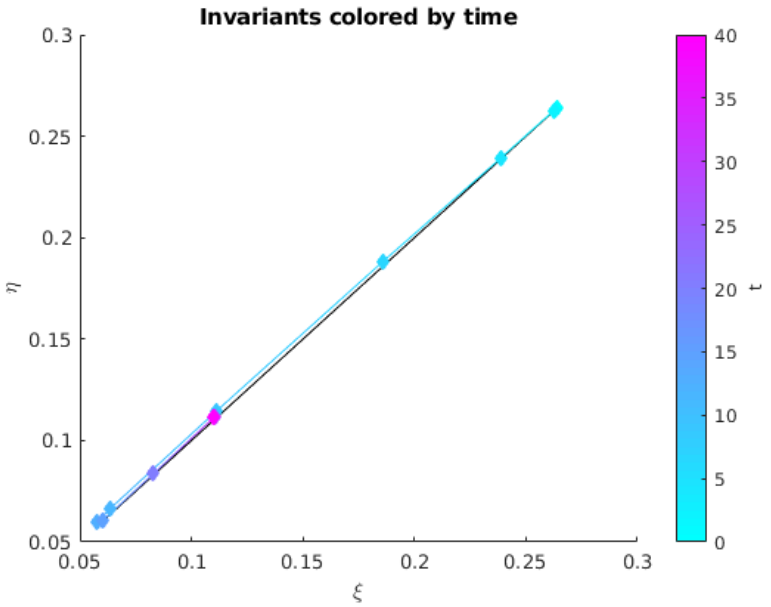

Figure 3: Invariants for the DNS

In Fig. 3, we can see the curve for Batchelor's similarity solution with fitted constants. To quantitively match Batchelor's solution would require nondimensionalization, which is not done here; the solution is merely scaled to give qualitative matches. The agreement for the TPE and TKE is as good as it was in [1]. This confirms that Batchelor's scaling is valid even in larger simulations and shows that this simulation is an ideal testbed for HVD.

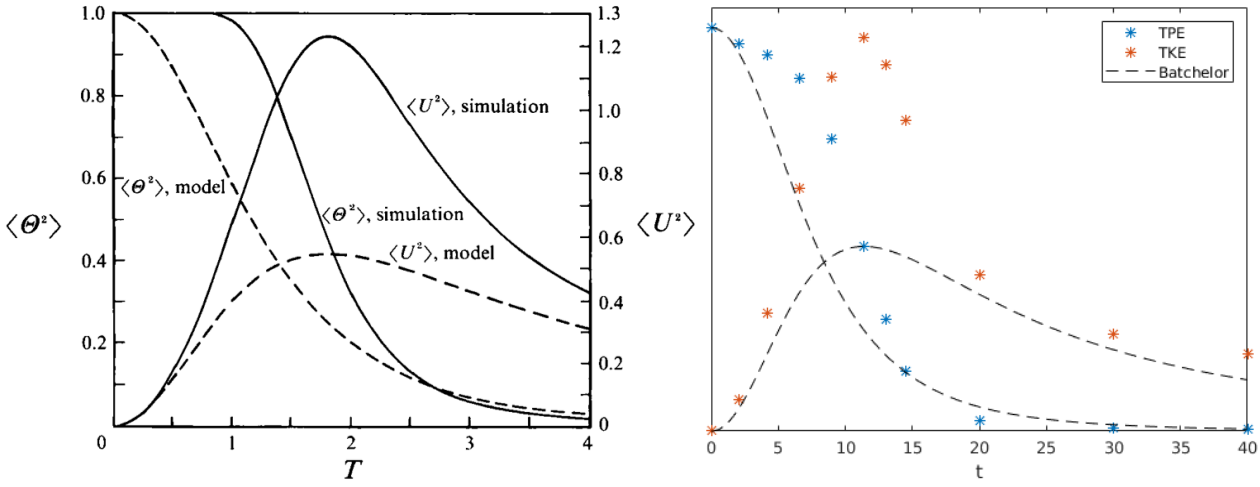

Figure 4: Computed (symbols) and theoretical (line) evolution of TPE and TKE against [1] (L)

Having gone through some theoretical work, now we can address LES models for closing the momentum equation of HVD flows. Because all data comes from a database, only static models that utilize the eddy viscosity hypothesis will be considered in this work, which is that:

$$< u_i u_j >^d = -2\nu_t \widetilde{D}_{ij} ,$$

where D_{ij} is the strain rate tensor and we only examine the deviatoric unresolved stresses.

In the atmospheric fluid dynamics literature, a common static model used is just the standard Smagorinsky model. According to [4], this model prescribes the eddy viscosity as

$$C_b = \begin{cases} \sqrt{1 - \frac{Ri}{Pr_t}} & \frac{Ri}{Pr_t} < 1 \\ 0 & \frac{Ri}{Pr_t} > 1 \end{cases} \qquad \nu_t = (C_s \Delta)^2 \left|\widetilde{D}\right| C_b$$

where Ri is the Richardson number, Pr_t is the turbulent Prandtl number of the flow, set to 0.5, and C_s is a constant equal to 0.2. When the Richardson number is below the stability limit, the model turns on according to the C_b parameter, following work by Mason.

[4] also proposes a modification of the standard Smagorinsky model which replaces the standard filter-width of the model with a mixing length, first used to handle the transport of TKE by Deardorff. If we assume the Richardson number used is the standard gradient Richardson number and N represents the standard Brunt–Väisälä frequency, then one can write this mixing length as:

$$L = \begin{cases} \frac{-\Delta}{c_2}\left(c_1\left(\frac{1}{Ri} - 1\right) - c_{e1}\right) & N^2 > 0 \\ \Delta & N^2 < 0 \end{cases}$$

This leads to a formulation of the eddy viscosity and related constants as:

$$C_b = \begin{cases} \sqrt{1 - \frac{Ri}{Pr_t}} & \frac{Ri}{Pr_t} < 1 \\ 0 & \frac{Ri}{Pr_t} > 1 \end{cases} \qquad \nu_t = \begin{cases} c_3 c_\epsilon^{-1/2} L^2 \left|\widetilde{D}\right| C_b & L > 0 \\ 0 & L < 0 \end{cases}$$

$$c_\epsilon = c_{e1} + \frac{c_{e2} L}{\Delta} \quad c_3 = c_a^{3/2} \quad c_{e1} = 0.19 \quad c_{e2} = 0.51 \quad c_a = 0.1 \quad c_2 = c_{e2} + 2c_1 \quad c_1 = c_a (0.76)^2$$

We can apply this model to the data from [3] using two filter widths. When we apply a top-hat filter with a width of 4 and 8 grid spacings, we see that the filtered invariants indicate that the flow reaches close to an isotropic condition for $t > 15$ for both filter widths, which was not observed in the DNS data. Models formulated for HIT should perform well here.

If we directly examine the diagonal Reynolds stresses, isotropy means the modified Smagorinsky model and the Deardorff-type model both perform well after the initial burst of energy injection

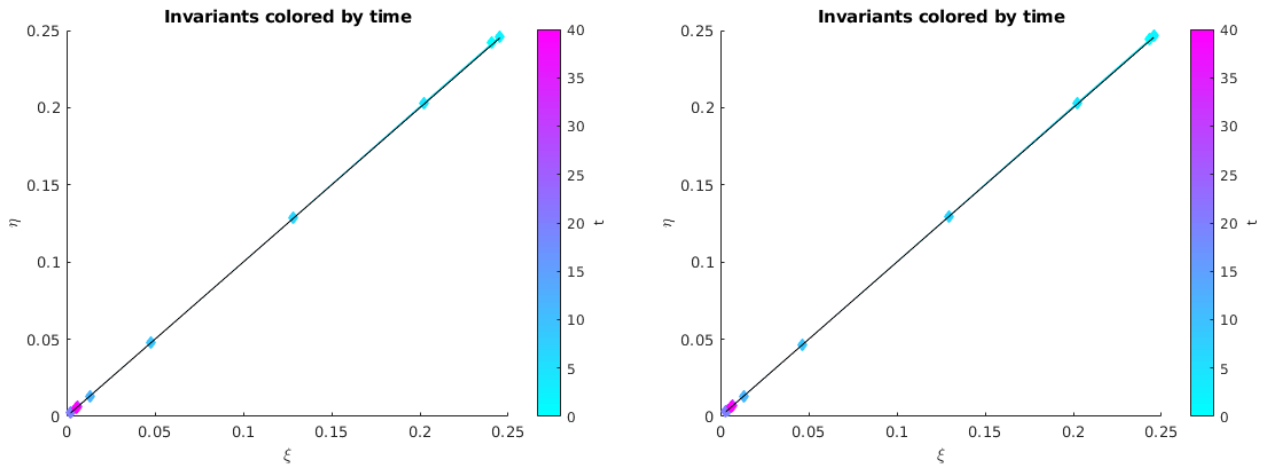

Figure 5: Invariants for the 4dx (L) and 8dx (R) filter widths

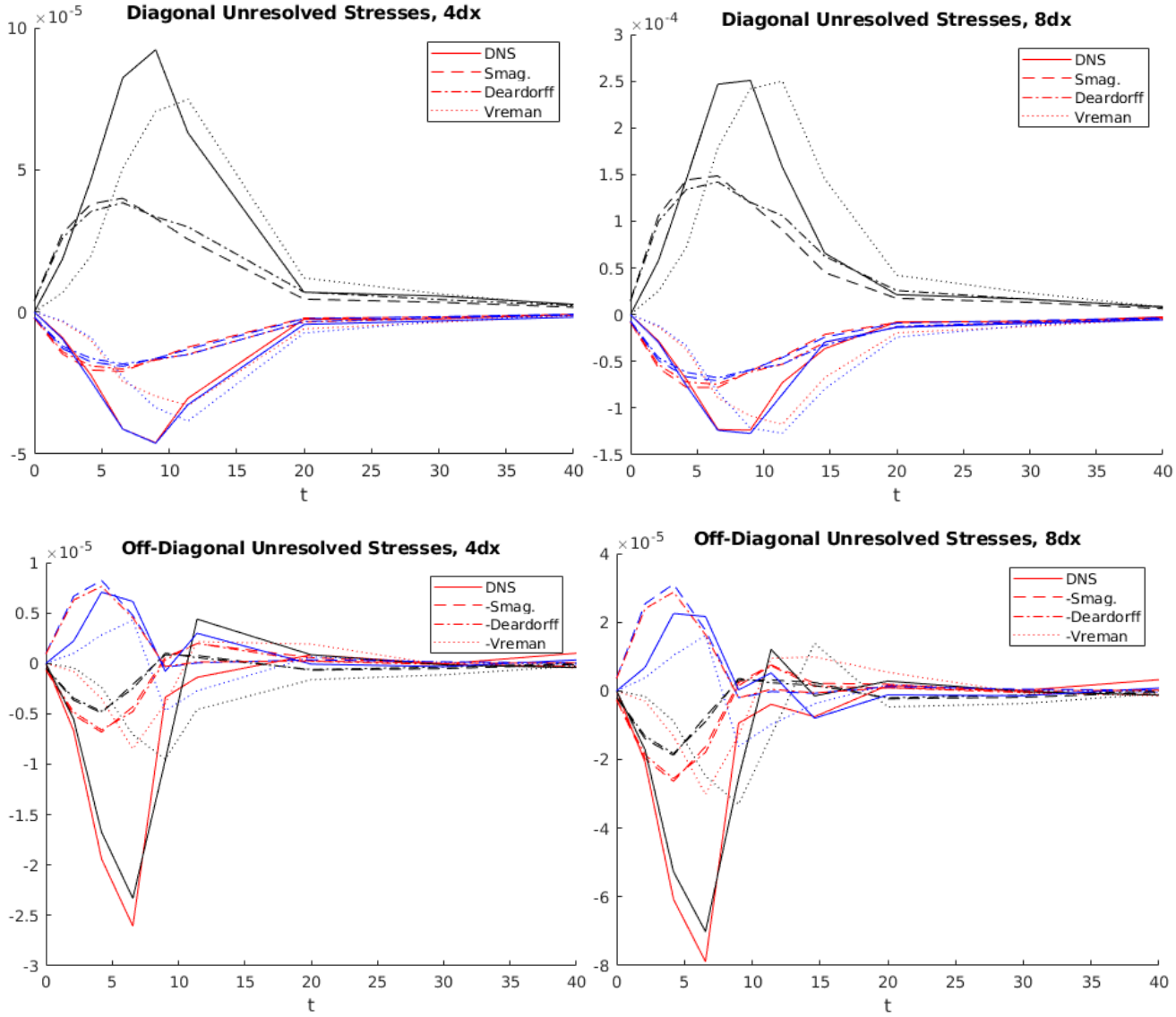

Figure 6: Unresolved stresses for the 4dx (L) and 8dx (R) cases

is over. The models perform fairly well in the approach to isotropy, but do not properly match the initial shear-produced values and miss the sign on the off-diagonal components, as can be seen in the legend of Fig. 6. If we are most concerned with the energetics of the flow, however, this last point is unimportant as the off-diagonal components are far smaller than the diagonal ones.

To combat the initial mismatch, a base model that better works in shear flows is needed. In particular, the fact that the Deardorff-type model offers improvements over the Smagorinsky model suggests the ability of that model to turn off when buoyant production is weak is a benefit. The Vreman model proposed in [5] is a good candidate for this observation. It uses invariants of the velocity gradient tensor to find a model form that has zero eddy viscosity when the flow is locally laminar. While not formulated for HVD flows, we can modify the original form by adding in the same Richardson number-based term used earlier to account for buoyancy effects as:

$$\nu_t = 2.5C_s^2\sqrt{\frac{B_\beta}{\alpha_{ij}\alpha_{ij}}}\,C_b$$

$$\alpha_{ij} = \frac{\partial U_j}{\partial x_i} \qquad \beta_{ij} = \Delta^2\alpha_{mi}\alpha_{mj} \qquad B_\beta = \beta_{11}\beta_{22} + \beta_{33}\beta_{22} + \beta_{11}\beta_{33} - \beta_{12}^2 - \beta_{23}^2 - \beta_{13}^2$$

where C_b is the factor proposed by Mason to added to the standard model.

In short, this model improves the prediction of the peak unclosed values, which neither of the previous models did. However, in the return to isotropy, the modified Vreman does not perform as well as the other two models that are commonly used. Partially, this may be from the choice of Smagorinsky constant; the value of 0.2 used is larger than the 0.17 usually prescribed for HIT. The fact that the corresponding profile better matches the DNS profile as the filter width increases is particularly salient for atmospheric models, which often under-resolve the inertial subrange.

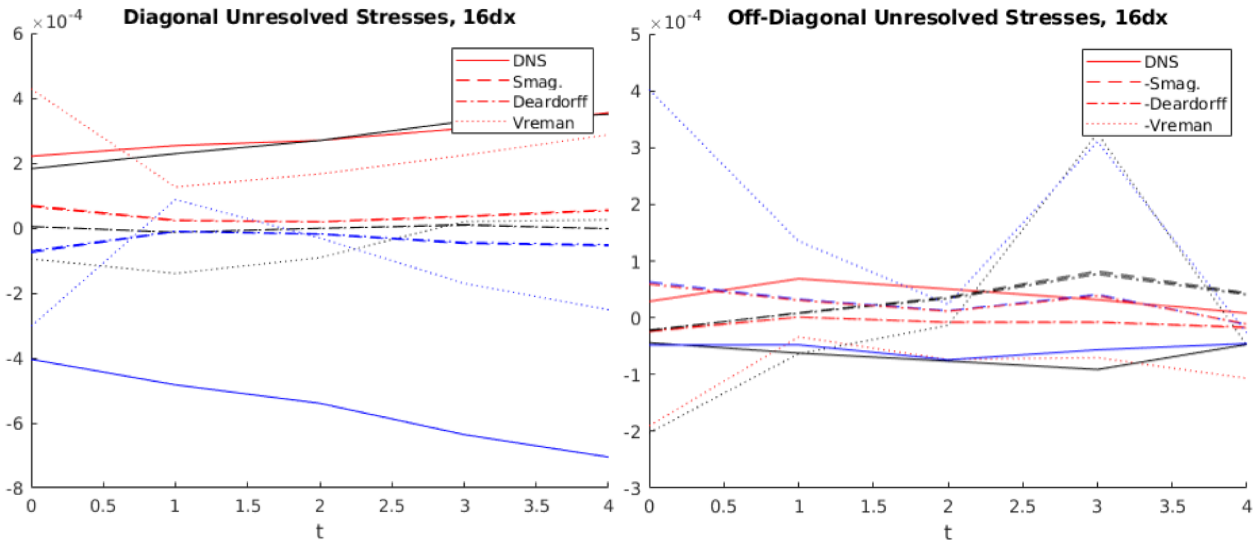

Figure 7: Unresolved stresses for the 16dx case of stratified, rotating turbulence

Based on a non-exhaustive literature review, these models have not been examined in this particular unsteady HVD scenario, so none of the parameters used except C_s are tuned for this case.

To apply the model to another canonical dataset and better reach the goal of simulating real geophysical flows, DNS data of rotating and stratified turbulence from the Johns Hopkins database in [6] was used. The identical models and parameters used earlier were used to predict the unresolved Reynolds stresses in Fig. 7, where we consider a system that is at steady state. We see that this flow is far from isotropic, as the off-diagonal components are of the same order of magnitude as the diagonal components, and the predicted values are far from the measured values for all models. This might be because the Rossby number of the flow is < 1, and as a geostrophic flow, we expect that the models used here, even in a Boussinesq context, won't capture sub-filter effects. The Coriolis terms are far more important, and as we are not modelling them, we cannot directly conclude anything about the applicability of the models proposed for stratified flows in this case.

A few models for capturing SGS stresses in HVD flow are tested in this project for two canonical cases. The HVD triply-periodic case, in particular, is a testbed that doesn't seem to have been used for this kind of model testing. With further time, doing *a posteriori* analysis of this problem using the three tested models would have been ideal, as would be the application of these models to a more realistic problem, such as the rotating, stratified turbulence of [6]. As no model tuning was performed in this project, it's possible that better performance might be obtained for either of the three models presented, and the use of a dynamic procedure could improve prediction as well. In particular, the Deardorff-type model uses parameters tuned for saturated air, which might be less suited than the standard Smagorinsky parameters for an imaginary fluid. Based purely on the analysis herein, however, a modified Vreman model might be a promising way to deal with HVD in practice if one doesn't want to use a dynamic procedure.

[1] Batchelor, G., Canuto, V., & Chasnov, J. (1992). Homogeneous buoyancy-generated turbulence. *Journal of Fluid Mechanics, 235*, 349-378.
[2] Livescu, D. & Ristorcelli, J. R. (2007) Buoyancy-driven variable-density turbulence. *Journal of Fluid Mechanics, 591*, 43–71.
[3] Livescu, D., Canada C., Kanov, K., Burns, R. & IDIES staff, J. Pulido, "Homogeneous Buoyancy driven turbulence data set"(2014), available at turbulence.pha.jhu.edu/docs/README-HBDT.pdf
[4] Kirkpatrick, M.P., A.S. Ackerman, D.E. Stevens, and N.N. Mansour (2006) On the Application of the Dynamic Smagorinsky Model to Large-Eddy Simulations of the Cloud-Topped Atmospheric Boundary Layer. *J. Atmos. Sci.*, *63*, 526–546.
[5] Vreman A. W. (2004) An eddy-viscosity subgrid-scale model for turbulent shear flow: Algebraic theory and applications. *Phys. Fluids 16*, 3670-3681.
[6] Rotating Stratified Turbulence Dataset on 4096^3 Grid: https://doi.org/10.7281/T1J964JJ